

# Nanocellulose Hybrids with Magnetic Nanoparticles

Subjects: Others

Contributor: Denis Mihaela Panaitescu, Madalina Oprea

Cellulose is one of the most affordable, sustainable and renewable resources, and has attracted much attention especially in the form of nanocellulose. Bacterial cellulose, cellulose nanocrystals or nanofibers may serve as a polymer support to enhance the effectiveness of metal nanoparticles. The resultant hybrids are valuable materials for biomedical applications due to the novel optical, electronic, magnetic and antibacterial properties. In particular, superparamagnetic iron oxides nanoparticles with very small size (SPIONs) are non-toxic in small concentration, biodegradable and biocompatible and display a high magnetic resonance imaging (MRI) contrast effect. However, for biomedical applications, SPIONs need to be covered by a biocompatible shell to prevent aggregation or degradation and to delay the immune response. Nanocellulose proved to be an excellent biocompatible matrix for SPIONs in MRI applications.

Keywords: bacterial cellulose ; iron oxides ; hybrids ; superparamagnetic ; contrast agents

---

## 1. Introduction

Cellulose is the most affordable, sustainable and renewable resource, which has attracted much attention in the last decades and stimulated researchers to develop cellulose-based materials with novel functions. Cellulosic materials with nanometer size at least in one dimension are referred to as nanocellulose. This nanomaterial is either isolated from plants or synthesized by bacteria. It shows high strength, low density, high crystallinity along with biodegradability and biocompatibility [1][2]. Nanocellulose is a very strong material, with a longitudinal Young's modulus exceeding 100 GPa and a transverse modulus between 10 and 50 GPa [3][4]. Due to its high stiffness, nanocellulose was largely used as a reinforcing agent for many polymer matrices. Good results were obtained in the case of nanocellulose reinforced biopolymers, due to their inherent low mechanical properties [2][4][5][6]. In addition, nanocellulose may serve as a polymer matrix for organic or inorganic agents in the form of nanoparticles, nanofibers or nanoplatelets [7][8]. Nanocellulose-based materials cover a huge range of applications, from biosensors, energy storage devices and flexible electronics to enzyme immobilization, wound healing, biodegradable packaging, CO<sub>2</sub> absorbent materials, water purification and oil recovery [2][8].

Nanocellulose may acquire new properties by combining with metal oxides. Due to their high surface energy, metal oxide nanoparticles (NPs) have an aggregation tendency when suspended in aqueous media or inserted in polymers [9]. A strategy for improving dispersion involves the use of nanocellulose as a supporting material for the fabrication of hybrids. Nanocellulose/iron oxides NPs hybrids showing magnetic or sensing properties are required in magnetic resonance imaging (MRI), tissue reconstruction or drug delivery [9]. A distinct class of metal oxides, superparamagnetic iron oxides nanoparticles with very small size (SPIONs), usually below 15 nm, is intensively studied for magnetically controllable drug delivery systems, cell labeling, biosensors and contrast agents for MRI [10]. SPIONs are non-toxic in small concentration, biodegradable and biocompatible and display a high MRI contrast effect. MRI is a non-invasive high spatial resolution technique for diagnostics, which measures the proton relaxation under an external magnetic field. SPIONs lead to the image contrast by dephasing the proton spin and decreasing of spin-spin relaxation time (T<sub>2</sub>). For biomedical applications, SPIONs need to be covered by a biocompatible shell to prevent aggregation or degradation and to delay the immune response [11]. According to recent studies, nanocellulose proved to be an excellent biocompatible matrix for SPIONs in MRI applications.

## 2. Nanocellulose Hybrids with Magnetic Nanoparticles

Hybrids consisting of cellulose and magnetic particles have attracted great interest in the biomedical field due to their advantages such as biocompatibility and biodegradability [12]. Iron oxides, particularly magnetite (Fe<sub>3</sub>O<sub>4</sub>), show superparamagnetic properties, high stability, low cost, good biocompatibility and low toxicity, which recommend them for magnetic biocomposites. Magnetic Fe<sub>3</sub>O<sub>4</sub> nanoparticles (Fe<sub>3</sub>O<sub>4</sub> NPs) have a demonstrated efficiency in magnetic resonance imaging, drug delivery, bio-separation, catalysis and wastewater cleaning. Their efficiency as well as physical

and chemical properties are influenced by their morphology, size and structure [13]. Currently applied techniques to synthesize metal oxides nanoparticles include thermal decomposition, co-precipitation and hydrothermal methods. Co-precipitation is usually preferred due to its simplicity, low temperature, time-saving, low cost and high quality of resulted iron oxide NPs [14].

## 2.1. Bacterial Cellulose/Iron Oxides Hybrids

Cerebral aneurysms are the most critical events in cerebral trauma and surgical conventional treatments have low success rate [15]. Pavon et al. developed an alternative technique for neuro-endovascular reconstruction [15][16][17]. They used a co-precipitation-based method to functionalize bacterial cellulose hydrogel with  $\text{Fe}_3\text{O}_4$  NPs. The materials were designed as coatings for the surface of metallic stents used for the reconstruction of tunica media tissue after a cerebral aneurysm. This novel process consists of arterial media reconstruction by using a stent covered with magnetic BC. Magnetic stimulation is used to orient magnetized endothelial cells, derived from the arterial wall or provided externally via a catheter, to the regions along the outer side of the BC/ $\text{Fe}_3\text{O}_4$ -covered stent. This method allows the growth of a new tissue over the device which closes the aneurysmal neck defect (Figure 1) [15]. Cellulose functionalization was performed by impregnating BC membranes with  $\text{FeCl}_3 \cdot 6\text{H}_2\text{O}$  and  $\text{FeCl}_2 \cdot 4\text{H}_2\text{O}$  solutions at 80 °C, under nitrogen flow and vigorous stirring accompanied by ammonium hydroxide ( $\text{NH}_4\text{OH}$ ) addition to form  $\text{Fe}_3\text{O}_4$  NPs inside the BC [16]. The surface of magnetic NPs used to develop magnetic materials for tissue regeneration should be modified for increased biocompatibility because plain magnetic NPs could cause genotoxicity and cells necrosis. Different solutions were tested for improving biocompatibility. In one attempt, oleic acid was added into the ferrofluid used for BC impregnation during the heating stage [17]. SEM images indicated that the magnetic NPs had an aggregation tendency, most likely due to the polar nature of fatty acid functional groups on their surface. In other attempts, polyethylene glycol (PEG), polyethyleneimine or citric acid were used to coat magnetic materials [15]. The nano-mechanical properties of neat BC and BC/ $\text{Fe}_3\text{O}_4$  were evaluated using in situ nano-indentation measurements in hydrated state. The stiffness range of the BC/ $\text{Fe}_3\text{O}_4$  hybrids (0.0025–0.04 GPa) was close to the values measured for both large arteries and veins of human cerebral vessels. A residual elastic straining effect similar to the one characteristic to biological tissues (e.g., tendons, blood vessels, ligaments) was also observed [17].

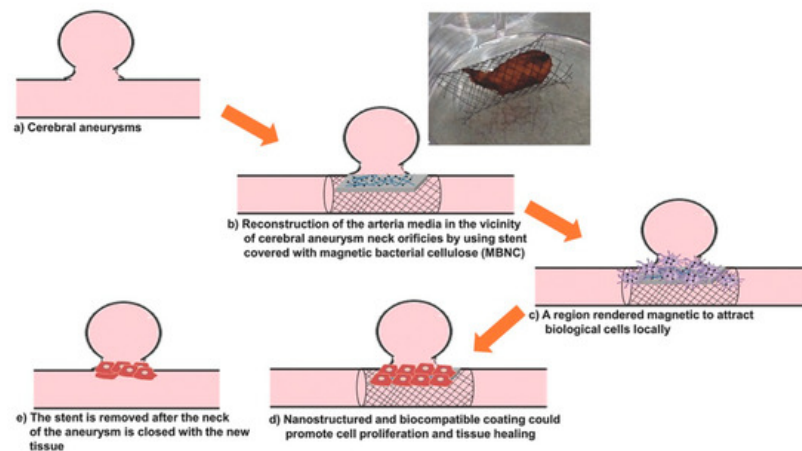


**Figure 1.** Stages of the blood vessel wall reconstruction process using stents covered with BC/ $\text{Fe}_3\text{O}_4$  hydrogel membranes; photograph of a Nitinol stent covered with magnetic BC, showing good adhesion properties [15].

Flexible magnetic BC nanohybrids were also obtained by in situ synthesis of  $\text{Fe}_3\text{O}_4$  NPs using ultrasonic irradiation and PEG as a coating polymer [18]. The results showed that ultrasonication and PEG ensured the homogeneous dispersion of  $\text{Fe}_3\text{O}_4$  NPs in the BC network. Moreover, the magnetic BC membranes obtained by this method showed a saturation magnetization of 40.58 emu/g and good mechanical properties.

## 2.2. Cellulose Nanocrystals/Iron Oxides Hybrids

Similarly to other metal oxides nanostructures [9],  $\text{Fe}_3\text{O}_4$  NPs can easily aggregate and oxidize in aqueous or oxygen environments, which limit their applications. To overcome these disadvantages, the surface of magnetic NPs can be modified with functional materials (e.g., mesoporous silica) to obtain core-shell structures with improved stability [19]. Another technique consists of the synthesis of  $\text{Fe}_3\text{O}_4$ -grafted cellulose nanocrystals. The negative charges, introduced in cellulose nanocrystals (CNC) structure during acid hydrolysis preparation process, generate an electrostatic repulsion among CNC- $\text{Fe}_3\text{O}_4$  particles, hence giving them the ability to effectively disperse in aqueous media [20].

MRI is a non-invasive clinical diagnostic technique used for anatomical imaging of soft body tissues. Contrast agents (CAs) are used to improve the image quality by shortening the relaxation time of water protons, thus increasing the MRI sensitivity [21]. Positive (T1) contrast agents reduce longitudinal relaxation time and produce brighter images, while negative (T2) ones shorten transverse relaxation time, resulting in darker images. The sensitivity of a contrast agent is defined by its relaxivity parameters (longitudinal— $r_1$  and transverse— $r_2$ ). The development of high-relaxivity CAs is desirable because they provide contrast enhancement at lower doses compared to low-relaxivity compounds, therefore the potential toxic effects are reduced [21][22][23]. Nanocellulose in the form of cellulose nanocrystals was used in combination with ultra-small superparamagnetic iron oxide nanoparticles (USPIONS) to develop a novel T1-T2 contrast agent [24]. Cellulose nanocrystals (CNC) were isolated from cotton linters using the acid-hydrolysis method, and incorporated in poly(citric acid) (PCA) to produce a biocompatible, dispersible and stable substrate. USPIONS magnetic nanoparticles were synthesized by thermal decomposition of iron (III) acetylacetonate precursor and loaded on the hydrophilic CNC-PCA substrate. To obtain the CNC-PCA/Fe<sub>3</sub>O<sub>4</sub> nanohybrids, predetermined quantities of USPIONS and CNC-PCA were separately dispersed in distilled water and ultrasonicated, then mixed for 24 h and dried in a vacuum oven [24]. FE-SEM images showed that the spherical Fe<sub>3</sub>O<sub>4</sub> NPs were well dispersed on the CNC-PCA surface and no aggregations were observed (Figure 2). The particle size distribution analyzed by dynamic light scattering showed that the average hydrodynamic size of Fe<sub>3</sub>O<sub>4</sub> NPs and CNC-PCA/Fe<sub>3</sub>O<sub>4</sub> was 13.2 and 12.0 nm, with a polydispersity index of 0.12 and 0.34.

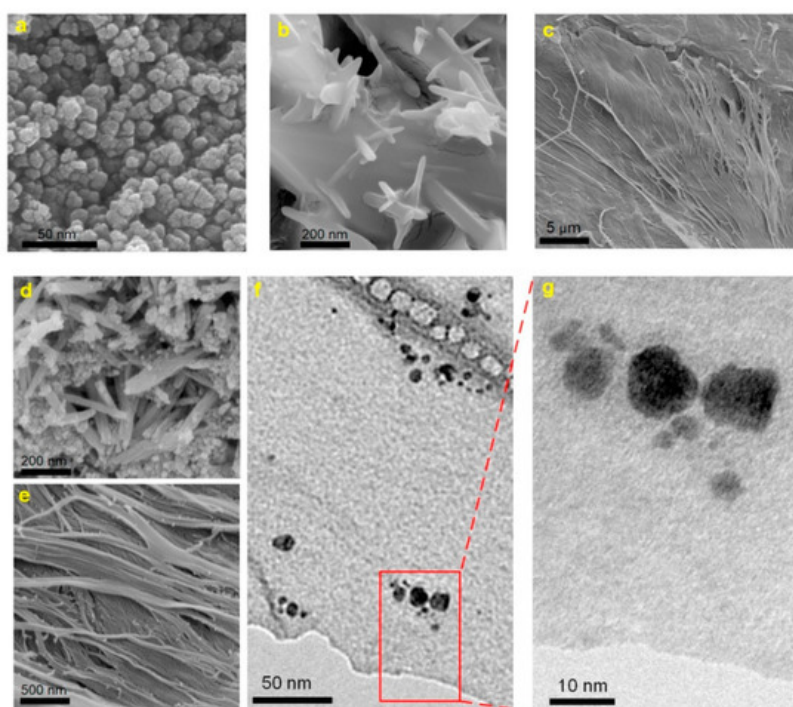


**Figure 2.** FE-SEM images of (a) Fe<sub>3</sub>O<sub>4</sub> NPs, (b, c) CNC-PCA and (d, e) CNC-PCA/Fe<sub>3</sub>O<sub>4</sub> hybrids, (f, g) TEM images of CNC-PCA/Fe<sub>3</sub>O<sub>4</sub> hybrids [24].

The XRD pattern of CNC-PCA/Fe<sub>3</sub>O<sub>4</sub> showed all the diffraction peaks corresponding to the crystal planes of Fe<sub>3</sub>O<sub>4</sub> and two new broad peaks at  $2\theta = 14.9^\circ$  and  $22.1^\circ$  associated to (110) and (002) planes in the structure of cellulose. The high saturation magnetization value ( $52.2 \text{ emu}\cdot\text{g}^{-1}$ ) and good relaxivity parameters  $r_1$  ( $13.8 \text{ mM}^{-1}\cdot\text{s}^{-1}$ ),  $r_2$  ( $96.2 \text{ mM}^{-1}\cdot\text{s}^{-1}$ ), obtained at 3.0 T magnetic field strength, demonstrated that the hybrids could be used successfully as dual MRI contrast agents (Figure 3). In addition, a higher iron concentration was associated with an enhanced signal intensity of T<sub>1</sub>-weighted images (brighter images) and a reduced signal intensity on T<sub>2</sub>-weighted images (darker images), the contrast being improved in both cases. In vitro cellular uptake was performed using inductively coupled plasma optical emission spectroscopy and in vitro cytotoxicity to HeLa cell lines was also investigated. The results revealed an appropriate cellular uptake, excellent biocompatibility and low toxicity, characteristics which make the CNC-PCA/Fe<sub>3</sub>O<sub>4</sub> nanohybrids promising for the intended biomedical application [24].

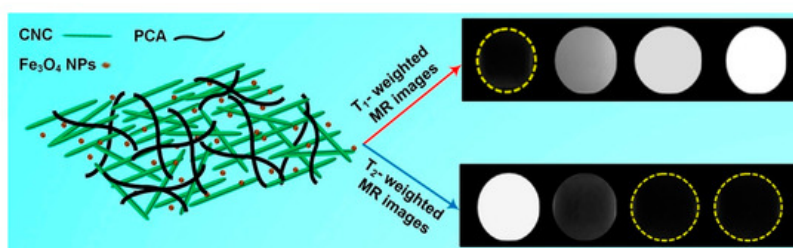


**Figure 3.** Schematic representation of the CNC-PCA/Fe<sub>3</sub>O<sub>4</sub> structure; T1- and T2-weighted MRI images of CNC-PCA/Fe<sub>3</sub>O<sub>4</sub> at increasing (left to right) Fe concentrations (0, 0.1, 0.3, 0.5 mM) [24].

Versatile magnetic materials based on cellulose nanocrystals and cobalt ferrite (CoFe<sub>2</sub>O<sub>4</sub>) were obtained by in situ synthesis of the inorganic nanoparticles on CNC support [25]. CNCs with length of approximately 150 nm were obtained from dry cotton by acid-hydrolysis. The magnetic nanomaterials were synthesized by treating CNC aqueous dispersions with precursor salts-ferrous (II) sulfate heptahydrate (FeSO<sub>4</sub>·7H<sub>2</sub>O) and cobalt chloride (CoCl<sub>2</sub>), followed by heat treatment. After the addition of the precipitating agents, NaOH and KNO<sub>3</sub>, the dispersion changed its color to brown, this being an indicator of CoFe<sub>2</sub>O<sub>4</sub> particles growth. CNC-CoFe<sub>2</sub>O<sub>4</sub> nanohybrids were further tested either as magneto-responsive dispersions or as precursors for self-standing films or composites nanofibers. The films could find applications in packaging and magnetic shielding and the composite nanofiber mats could be considered for magnetic separation procedures [25]. The amount of inorganic nanoparticles in CNC-CoFe<sub>2</sub>O<sub>4</sub> nanohybrids was verified by the residue at 800 °C in TGA measurements. FE-SEM-EDX analysis of CNC-CoFe<sub>2</sub>O<sub>4</sub> dispersion showed that the inorganic NPs were mainly spherical with diameter of approximately 10–40 nm. The hybrid dispersion was stable, CNCs being able to function as a nucleation site for the inorganic particle growth and also as a stabilizing network. Preliminary studies regarding the utilization of the aqueous CNC-CoFe<sub>2</sub>O<sub>4</sub> dispersion in magnetic hyperthermia were conducted and an increase with 8 °C of the temperature (from 24 to 32 °C) was achieved in 40 min. This effect may be improved by using a higher magnetic NPs loading [25].

### 3. Influence of Metal Oxide NPs on the Properties of Cellulose Nanohybrids

Besides magnetic nanoparticles, other types of metal oxides were also combined with nanocellulose to obtain improved hybrid materials for biomedical applications. A summary of nanocellulose-metal oxide nanocomposites studied for biomedical applications [26][27][28][29][30][31][32][33][34][35][36][37][38] is presented in Table 1. The magnetic properties of nanocellulose-metal oxide nanohybrids were presented in the previous chapter along with the methods of obtaining these nanohybrids. Iron oxide NPs can also influence their thermal and mechanical properties, which are important for the biomedical applications of these nanohybrids. BC shows a major degradation step between 250 and 375 °C, with a maximum degradation rate temperature around 320 °C [28][30][39]. This is due to the dehydration, depolymerization and decomposition of glucose units.

**Table 1.** Various types of metal oxides incorporated in nanocellulose to obtain functional hybrids for biomedical applications.

Nr.	Nano-Cellulose	Metal Oxide NPs	Nanocomposite Preparation Method	Application	Ref.
1.	BC	ZnO	Ex situ synthesis of NPs, immersion of BC membrane and mixing	Wound dressing systems in burns complication	[26]
2.	BC	ZnO	MAPLE	Wound dressing materials	[27]
3.	BC	ZnO	Ex situ synthesis of NPs and mixing with BC dissolved in NMMO	Biomedical applications and bioelectroanalysis	[28]

4.	BC	ZnO	Ultrasonic-assisted in situ synthesis of NPs inside the BC template	Active antibacterial wound dressing	[29]
5.	BC	ZnO	Single-pot method: BC impregnation in NPs precursor	Wound healing	[30]
6.	BC	ZnO	SPP synthesis and deposition of NPs into BC pellicles	Antibacterial material in wound dressing	[31]
7.	BC	ZnO	BC modified with maleic anhydride template for in situ synthesis of NPs	Antibacterial wound dressing and tissue regeneration	[32]
8.	BC	TiO <sub>2</sub>	Ex situ sol-gel method	Antibacterial and photocatalytic applications	[33]
9.	BC	TiO <sub>2</sub>	Ex situ synthesis of NPs and mixing with BC dissolved in NMMO	Wound healing and tissue regeneration	[34]
10.	BC	CuO	GO-CuO nanohybrids blended with homogenized BC	Biomedical applications	[35]
11.	BC	MgO	Nanohybrids obtained by in situ co-precipitation method and ex situ incorporation of MgO-NPs in the BC	Clinical wound healing	[36]

12.	CNC	ZnO	Sheet-like CNC-ZnO nanohybrids by one-step hydrothermal method	Wound dressing	[37]
13.	CNF	Cu/ CuO	In situ generation of Cu/CuO NPs using green reductive technique and coating CNF	Surgical bandage material	[38]
14.	BC	Fe <sub>3</sub> O <sub>4</sub>	In situ generation of Fe <sub>3</sub> O <sub>4</sub> NPs inside the BC network in the presence of oleic acid or PEG	Tissue reconstruction at the cerebral aneurysmal neck defect	[15] [16] [17]
15.	CNC	Fe <sub>3</sub> O <sub>4</sub>	Ex situ generation of Fe <sub>3</sub> O <sub>4</sub> and mixing with CNC-poly(citric acid) by ultrasonication	Dual contrast agent for MRI in biomedical applications	[24]
16.	CNC	CoFe <sub>2</sub> O <sub>4</sub>	In situ synthesis of CoFe <sub>2</sub> O <sub>4</sub> NPs starting from precursor salts in the presence of CNC	Magnetic fluid hyperthermia, magnetically assisted drug delivery	[25]

A significant increase of thermal stability, with more than 50 °C, was noticed in the case of BC/Fe<sub>3</sub>O<sub>4</sub> nanocomposites with a high proportion of magnetic nanoparticles [18]. The composition and preparation conditions influenced the thermal behavior. Thus, the method involving ultrasonication led to a smaller increase of the thermal stability than the one without ultrasound irradiation due to the disruption of the BC network that decreased its crystallinity [18]. Moreover, BC/Fe<sub>3</sub>O<sub>4</sub> hybrids showed excellent flexibility, the repeated bending through 360° caused no apparent damage [18]. Furthermore, it was found that the addition of Fe<sub>3</sub>O<sub>4</sub> NPs in BC hydrogels resulted in the outer surface reduction of both hardness and E values, compared to the neat BC samples [17]. This was explained by the inhibiting effect of magnetic NPs attached to BC nanofibers on the hydrogen bonding mechanism. Finally, it was observed that the mechanical properties of BC/Fe<sub>3</sub>O<sub>4</sub> hybrids fall within the required range for the intended biomedical application (0.0025–0.04 GPa) [17].

## References

1. Kargarzadeh, H.; Mariano, M.; Gopakumar, D.; Ahmad, I.; Thomas, S.; Dufresne, A.; Huang, J.; Lin, N. Advances in cellulose nanomaterials. *Cellulose* 2018, 25, 2151-2189.
2. Siqueira, G.; Bras, J.; Dufresne, A. Cellulosic bionanocomposites: a review of preparation, properties and applications. *Polymers* 2010, 2, 728-765.
3. Šturcová, A.; Davies, G.R.; Eichhorn, S.J. Elastic modulus and stress-transfer properties of tunicate cellulose whiskers. *Biomacromolecules* 2005, 6, 1055-1061.
4. Panaitescu, D.M.; Frone, A.N.; Ghiurea, M.; Chiulan, I. Influence of storage conditions on starch/PVA films containing cellulose nanofibers. *Ind. Crops Prod.* 2015, 70, 170-177.
5. Kargarzadeh, H.; Huang, J.; Lin, N.; Ahmad, I.; Mariano, M.; Dufresne, A.; Thomas, S.; Gałęski, A. Recent developments in nanocellulose-based biodegradable polymers, thermoplastic polymers, and porous nanocomposites. *Prog. Polym. Sci.* 2018, 87, 197-227.
6. Panaitescu, D.M.; Frone, A.N.; Chiulan, I. Nanostructured biocomposites from aliphatic polyesters and bacterial cellulose. *Ind. Crops Prod.* 2016, 93, 251-266.
7. Farooq, A.; Patoary, M.K.; Zhang, M.; Mussana, H.; Li, M.; Naeem, M.A.; Mushtaq, M.; Farooq, A.; Liu, L. Cellulose from sources to nanocellulose and an overview of synthesis and properties of nanocellulose/zinc oxide nanocomposite materials. *Int. J. Biol. Macromol.* 2020, 154, 1050-1073, doi:<https://doi.org/10.1016/j.ijbiomac.2020.03.163>.
8. Zhang, Q.; Zhang, L.; Wu, W.; Xiao, H. Methods and applications of nanocellulose loaded with inorganic nanomaterials: A review. *Carbohydr. Polym.* 2020, 229, 115454.
9. Wells, M.A.; Abid, A.; Kennedy, I.M.; Barakat, A.I. Serum proteins prevent aggregation of Fe<sub>2</sub>O<sub>3</sub> and ZnO nanoparticles. *Nanotoxicology* 2012, 6, 837-846.
10. Abo-zeid, Y.; Williams, G.R. The potential anti-infective applications of metal oxide nanoparticles: A systematic review. *Wiley Interdiscip. Rev. Nanomed. Nanobiotech.* 2020, 12, e1592.
11. Hola, K.; Markova, Z.; Zoppellaro, G.; Tucek, J.; Zboril, R. Tailored functionalization of iron oxide nanoparticles for MRI, drug delivery, magnetic separation and immobilization of biosubstances. *Biotech. Adv.* 2015, 33, 1162-1176, doi:[10.1016/j.biotechadv.2015.02.003](https://doi.org/10.1016/j.biotechadv.2015.02.003).
12. Furlan, D.M.; Morgado, D.L.; Oliveira, A.J.A.d.; Faceto, Â.D.; Moraes, D.A.d.; Varanda, L.C.; Frollini, E. Sisal cellulose and magnetite nanoparticles: formation and properties of magnetic hybrid films. *J. Mater. Res. Technol.* 2019, 8, 2170-2179, doi:<https://doi.org/10.1016/j.jmrt.2019.02.005>.
13. Cotin, G.; Piant, S.; Mertz, D.; Felder-Flesch, D.; Begin-Colin, S. Chapter 2 - Iron Oxide Nanoparticles for Biomedical Applications: Synthesis, Functionalization, and Application. In *Iron Oxide Nanoparticles for Biomedical Applications*, Mahmoudi, M., Laurent, S., Eds. Elsevier: 2018, pp. 43-88, <https://doi.org/10.1016/B978-0-08-101925-2.00002-4>.
14. Xiong, R.; Wang, Y.; Zhang, X.; Lu, C. Facile synthesis of magnetic nanocomposites of cellulose@ultra-small iron oxide nanoparticles for water treatment. *RSC Adv.* 2014, 4, 22632-22641, doi:[10.1039/C4RA01397B](https://doi.org/10.1039/C4RA01397B).
15. Echeverry-Rendon, M.N.; Reece, L.; Pastrana, H.; Arias, S.; Shetty, A.; Pavón, J.; Allain, J.P. Bacterial Nanocellulose Magnetically Functionalized for Neuro-Endovascular Treatment. *Macromol. Biosci.* 2017, 17, 1600382, doi:[10.1002/mabi.201600382](https://doi.org/10.1002/mabi.201600382).
16. Arias, S.L.; Shetty, A.R.; Senpan, A.; Echeverry-Rendón, M.; Reece, L.M.; Allain, J.P. Fabrication of a Functionalized Magnetic Bacterial Nanocellulose with Iron Oxide Nanoparticles. *J. Vis. Exp.* 2016, 10.3791/52951, 52951, doi:[10.3791/52951](https://doi.org/10.3791/52951).
17. Pavón, J.J.; Allain, J.P.; Verma, D.; Echeverry-Rendón, M.; Cooper, C.L.; Reece, L.M.; Shetty, A.R.; Tomar, V. In situ Study Unravels Bio-Nanomechanical Behavior in a Magnetic Bacterial Nano-cellulose (MBNC) Hydrogel for Neuro-Endovascular Reconstruction. *Macromol. Biosci.* 2019, 19, 1800225, doi:[10.1002/mabi.201800225](https://doi.org/10.1002/mabi.201800225).
18. Zheng, Y.; Yang, J.; Zheng, W.; Wang, X.; Xiang, C.; Tang, L.; Zhang, W.; Chen, S.; Wang, H. Synthesis of flexible magnetic nanohybrid based on bacterial cellulose under ultrasonic irradiation, *Mat. Sci. Eng. C* 2013, 33(4), 2407-2412.
19. Buchman, J.T.; Pho, T.; Rodriguez, R.S.; Feng, Z.V.; Haynes, C.L. Coating iron oxide nanoparticles with mesoporous silica reduces their interaction and impact on *S. oneidensis* MR-1. *Chemosphere* 2019, 237, 124511, doi:<https://doi.org/10.1016/j.chemosphere.2019.124511>.
20. Ren, S.; Zhang, X.; Dong, L.; Lei, T.; Teng, Z.; Song, K.; Sun, X.; Wu, Q. Cellulose nanocrystal supported superparamagnetic nanorods with aminated silica shell: synthesis and properties. *J. Mater. Sci.* 2017, 52, 6432-6441.

21. Beato-López, J.J.; Domínguez, M.; Ramírez-del-Solar, M.; Litrán, R. Glutathione-magnetite nanoparticles: synthesis and physical characterization for application as MRI contrast agent. *SN Appl. Sci.* 2020, 2, 1202, doi:10.1007/s42452-020-3010-y.
22. Yim, H.; Seo, S.; Na, K. MRI Contrast Agent-Based Multifunctional Materials: Diagnosis and Therapy. *J. Nanomater.* 2011, 2011, 747196, doi:10.1155/2011/747196.
23. Jacques, V.; Dumas, S.; Sun, W.C.; Troughton, J.S.; Greenfield, M.T.; Caravan, P. High-relaxivity magnetic resonance imaging contrast agents. Part 2. Optimization of inner- and second-sphere relaxivity. *Invest. Radiol.* 2010, 45(10), 613–624, <https://doi.org/10.1097/RLI.0b013e3181ee6a49>.
24. Torkashvand, N.; Sarlak, N. Fabrication of a dual T1 and T2 contrast agent for magnetic resonance imaging using cellulose nanocrystals/Fe3O4 nanocomposite. *Eur. Polym. J.* 2019, 118, 128-136, doi:<https://doi.org/10.1016/j.eurpolymj.2019.05.048>.
25. Nypelö, T.; Rodriguez-Abreu, C.; Rivas, J.; Dickey, M.D.; Rojas, O.J. Magneto-responsive hybrid materials based on cellulose nanocrystals. *Cellulose* 2014, 21, 2557-2566.
26. Khalid, A.; Khan, R.; Ul-Islam, M.; Khan, T.; Wahid, F. Bacterial cellulose-zinc oxide nanocomposites as a novel dressing system for burn wounds. *Carbohydr. Polym.* 2017, 164, 214-221, doi:<https://doi.org/10.1016/j.carbpol.2017.01.061>.
27. Dincă, V.; Mocanu, A.; Isopencu, G.; Busuioc, C.; Brajnicov, S.; Vlad, A.; Icriverzi, M.; Roseanu, A.; Dinescu, M.; Stroescu, M., et al. Biocompatible pure ZnO nanoparticles-3D bacterial cellulose biointerfaces with antibacterial properties. *Arab. J. Chem.* 2020, 13, 3521-3533, doi:<https://doi.org/10.1016/j.arabjc.2018.12.003>.
28. Ul-Islam, M.; Khattak, W.A.; Ullah, M.W.; Khan, S.; Park, J.K. Synthesis of regenerated bacterial cellulose-zinc oxide nanocomposite films for biomedical applications. *Cellulose* 2014, 21, 433-447, doi:10.1007/s10570-013-0109-y.
29. Katepetch, C.; Rujiravanit, R.; Tamura, H. Formation of nanocrystalline ZnO particles into bacterial cellulose pellicle by ultrasonic-assisted in situ synthesis. *Cellulose* 2013, 20, 1275-1292, doi:10.1007/s10570-013-9892-8.
30. Wahid, F.; Duan, Y.-X.; Hu, X.-H.; Chu, L.-Q.; Jia, S.-R.; Cui, J.-D.; Zhong, C. A facile construction of bacterial cellulose/ZnO nanocomposite films and their photocatalytic and antibacterial properties. *Int. J. Biol. Macromol.* 2019, 132, 692-700, doi:<https://doi.org/10.1016/j.ijbiomac.2019.03.240>.
31. Janpetch, N.; Saito, N.; Rujiravanit, R. Fabrication of bacterial cellulose-ZnO composite via solution plasma process for antibacterial applications. *Carbohydr. Polym.* 2016, 148, 335-344, doi:<https://doi.org/10.1016/j.carbpol.2016.04.066>.
32. Luo, Z.; Liu, J.; Lin, H.; Ren, X.; Tian, H.; Liang, Y.; Wang, W.; Wang, Y.; Yin, M.; Huang, Y., et al. In situ Fabrication of Nano ZnO/BCM Biocomposite Based on MA Modified Bacterial Cellulose Membrane for Antibacterial and Wound Healing. *Int. J. Nanomed.* 2020, 15, 1-15, doi:10.2147/IJN.S231556.
33. Brandes, R.; de Souza, L.; Vargas, V.; Oliveira, E.; Mikowski, A.; Carminatti, C.; Al-Qureshi, H.; Recouvreux, D. Preparation and characterization of bacterial cellulose/TiO2 hydrogel nanocomposite. *J. Nano Res.* 2016, 43, 73-80.
34. Khan, S.; Ul-Islam, M.; Khattak, W.A.; Ullah, M.W.; Park, J.K.J.C. Bacterial cellulose-titanium dioxide nanocomposites: nanostructural characteristics, antibacterial mechanism, and biocompatibility. *Cellulose* 2015, 22, 565-579.
35. Xie, Y.-Y.; Hu, X.-H.; Zhang, Y.-W.; Wahid, F.; Chu, L.-Q.; Jia, S.-R.; Zhong, C. Development and antibacterial activities of bacterial cellulose/graphene oxide-CuO nanocomposite films. *Carbohydr. Polym.* 2020, 229, 115456, doi:<https://doi.org/10.1016/j.carbpol.2019.115456>.
36. Mirtalebi, S.S.; Almasi, H.; Khaledabad, M.A.; Physical, morphological, antimicrobial and release properties of novel MgO-bacterial cellulose nanohybrids prepared by in-situ and ex-situ methods, *Int. J. Biol. Macromol.* 2019, 128, 848-857.
37. Abdalkarim, S.; Yu, H.; Wang, C.; Yang, L.; Guan, Y.; Huang, L.; Yao, J. Sheet-like cellulose nanocrystal-ZnO nanohybrids as multifunctional reinforcing agents in biopolyester composite nanofibers with ultrahigh UV-Shielding and antibacterial performances. *ACS Appl. Bio Mater.* 2018, 1(3), 10.1021/acsabm.8b00188, doi:10.1021/acsabm.8b00188.
38. Barua, S.; Das, G.; Aidew, L.; Buragohain, A.; Karak, N. Copper-copper oxide coated nanofibrillar cellulose: A promising biomaterial. *RSC Adv.* 2013, 3, doi:10.1039/C3RA42209G.
39. Oprea, M.; Panaitescu, D.M.; Nicolae, C.A.; Gabor, A.R.; Frone, A.N.; Raditoiu, V.; Trusca, R.; Casarica, A. Nanocomposites from functionalized bacterial cellulose and poly(3-hydroxybutyrate-co-3-hydroxyvalerate). *Polym. Degrad. Stab.* 2020, 179, 109203, doi:<https://doi.org/10.1016/j.polymdegradstab.2020.109203>.

